The 'hidden story' in simulating reflected radiance by wind-roughened sea surface: Mobley's 1999 paper on simulation of R_{rs} measurements via the above-surface approach

Zhongping Lee [1], Xiaodong Zhang [2]

[1] State Key Lab of Marine Environmental Science, College of Ocean and Earth Sciences, Xiamen University, Xiamen, China

[2] Division of Marine Sciences, School of Ocean Science and Engineering, the University of Southern Mississippi, USA

Abstract

Remote sensing reflectance (R_{rs}, in sr^{-1}) is defined as the ratio of water-leaving radiance (L_w) to downwelling irradiance just above the water surface (E_s). To measure R_{rs}, the above-water approach (AWA) is a widely adopted scheme in the past decades. In addition to the measurement of E_s, AWA also involves measurements of upwelling radiance above the surface (L_t) and downwelling sky radiance (L_{sky}), with the latter component utilized for the removal of surface-reflected skylight (L_{sky}) or sky glint (L_{srs}), as L_t always contains both L_w and L_{srs}. In this classical paper (Applied Optics, 1999, Vol. 38, pp. 7442-7455), Mobley applied the widely-used Hydrolight to simulate L_t, L_w, and L_{sky} for various Sun-sensor geometries, wind speeds, and cloud cover. With Monte Carlo simulations, Mobley also showed that a roughened sea surface would reflect incident L_{sky} into a sensor's field-of-view (FOV) from an area much wider than that constrained by the FOV, which greatly helped understanding the difficulties in obtaining accurate R_{rs} in field measurements via AWA. Based on the simulations, Mobley concluded that "until an improved method of estimating *R*rs becomes available and accepted, the following suggestions can be made for using the traditional method based on Eq. (6)." This "Eq. (6)" is Eq. 4 below, and the suggestions include 1) an overall value of 0.028 for the surface reflectance (ρ) for a wind speed less than 5 m/s, and 2) an optimal viewing geometry of 40°/135°, with 40° for senor's nadir viewing angle and 135° for sensor's azimuth angle from the Sun. This paper has greatly impacted ocean color sciences, as these recommendations have been followed globally in the past two decades and today. However, there are a few 'hidden stories' in these simulations that were not disclosed or well discussed, and these hidden features put the suggestions in question.

1. Background

Above-water approach (AWA) usually employs a well calibrated graycard for the determination of E_s, which can be expressed as

$$E_s = \frac{\pi L_g}{R_g} \tag{1}$$

Here L_g is the radiance above the graycard after reflecting incident E_s, with R_g the card's reflectance, and the graycard is assumed as a Lambertian reflector. Thus, as long as R_g is known, E_s can be obtained when L_g is measured.

However, it is very complicated for AWA to accurately determinate L_w. As emphasized in Mobley [1], the measured L_t is a sum of L_w and surface-reflected radiance (L_{srs}), which can be written as

$$L_t(\theta_{v,w}, \varphi) = L_w(\theta_{v,w}, \varphi) + L_{srs}(\theta_{v,w}, \varphi) \tag{2a}$$

$$L_{srs}(\theta_{v,w}, \varphi) = \sum W_i \, f_i \, L_{sky-i} \tag{2b}$$

Here $\theta_{v,w}$ is sensor's view angle from nadir, φ is sensor's azimuth angle from the solar plane. W_i is the fraction of the ith facet of waves reflecting sky light, f_i the Fresnel Reflectance of this facet, and L_{sky-i} the sky radiance corresponding to the ith facet that is reflected into sensor's FOV. Assume L_{sky-i} can be precisely measured using a fisheye-type radiometer, it is difficulty, if not impossible, to determine W_i for a dynamic, wave-roughened, sea surface. As a result, Eq. 2 is not applicable for the determination of L_w. To be workable, as in Mobley [1], many studies simplified the above equation as

$$L_t(\theta_{v,w}, \varphi) = L_w(\theta_{v,w}, \varphi) + \rho(\theta_{v,w}, \varphi) L_{sky}(\theta_{v,s}, \varphi) \tag{3}$$

with ρ an averaged sea-surface reflectance corresponding to $L_{sky}(\theta_{v,s})$. Here $\theta_{v,s}$ is the reciprocal angle of $\theta_{v,w}$, thus $\theta_{v,s} = \theta_{v,w}$ in values, except that $\theta_{v,w}$ is in reference to nadir while $\theta_{v,s}$ is in reference to zenith. Following the definition of R_{rs}, it can then be calculated as

$$R_{rs}(\theta_{v,w}) = \frac{R_g}{\pi} \frac{\left(L_t(\theta_{v,w}) - \rho(\theta_{v,w}) L_{sky}(\theta_{v,s}) \right)}{L_g} \tag{4}$$

Since L_g, $L_t(\theta_{v,w},\phi)$ and $L_{sky}(\theta_{v,s},\phi)$ can all be measured with a spectroradiometer, thus R_{rs} can be handily calculated from Eq. 4 if the value of ρ is known. Further, if the same sensor is used to measure the three properties, the sensor does not have to be radiometrically calibrated to obtain R_{rs}, as long as this sensor's response is linearly proportional to the radiance energy.

The challenge in calculating R_{rs} from Eq. 4 is in the determination of the value of ρ, where the product of ρL_{sky} is equivalent or greater than L_w for most natural waters, thus an error or uncertainty in ρ will greatly affect the accuracy of R_{rs}. Therefore, it is important to have a good understanding on the variation of ρ values. On the other hand, because the roughened sea surface brings sky radiance from a big portion of the sky (see Fig. 2 of Mobley [1]), and that the sky radiance is not uniform, the value of ρ in Eq. 3 and Eq. 4 could not be determined analytically. Numerical simulations, as indicated in Mobley [1], is likely the only feasible way at present to analyze ρ, which is the objective of Mobley [1]. Further, from the simulations, Mobley [1] provided suggestions as mentioned above.

2. The 'hidden story'

Based on Eq. 2 and Eq. 3, the effective surface reflectance (ρ) is (expressions in integration form can be found in Mobley [1] and Zhang et al. [2])

$$\rho(\lambda, \theta_{v,w}, \varphi) = \frac{\sum W_i f_i L_{sky}(\lambda,\theta_i,\varphi_i)}{L_{sky}(\lambda,\theta_{v,s},\varphi)} \quad (5)$$

with (θ_i,φ_i) representing the direction of $L_{sky\text{-}i}$ reflected by the ith facet into the sensor's FOV. Note that here we include the wavelength variable (λ) in the expressions, as radiance is always wavelength dependent. Eq. 5 indicates that an accurate analysis and evaluation of ρ requires a precise simulation of $L_{sky}(\lambda)$ in the sky dome as well as an appropriate simulation of W_i (f_i can be adequately calculated for any given incident or viewing angle). Did the simulations in Mobley [1] meet these requirements?

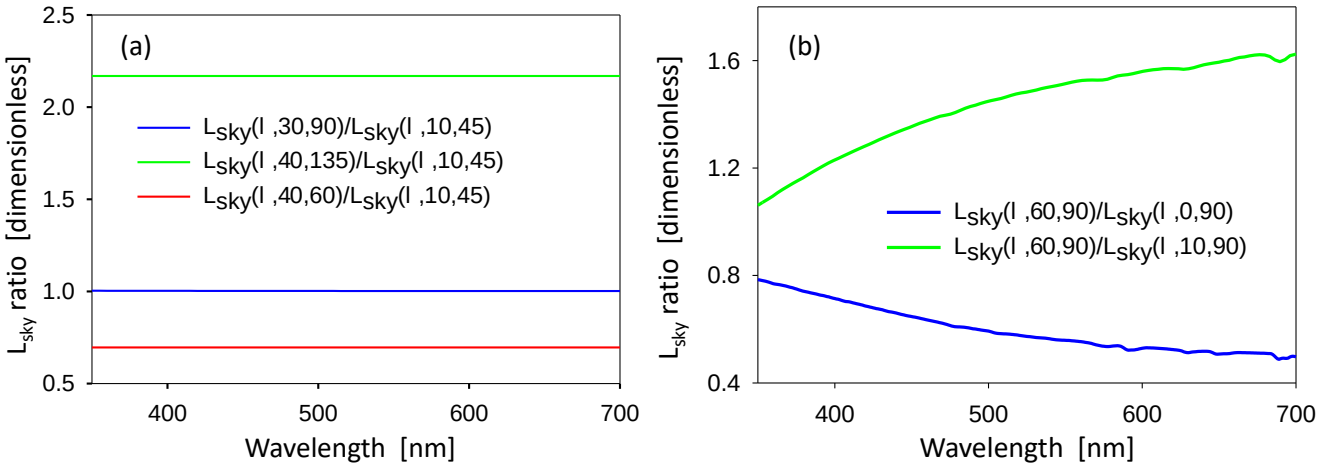

Fig. 1. (a) Spectra of $L_{sky}(\lambda,\theta_1,\varphi_1)/L_{sky}(\lambda,\theta_2,\varphi_2)$ from Hydrolight simulations for Sun at 30° from zenith. (b) Spectra of $L_{sky}(\lambda,\theta_1,\varphi_1)/L_{sky}(\lambda,\theta_2,\varphi_2)$ measured with solar zenith angle around 30° in Xiamen, Fujian, China (blue line) and with solar zenith angle around 50° in Qingdao, Shandong, China (green line). The values of θ_1,φ_1, θ_2,φ_2 are shown in the legend.

a) Simulation of $L_{sky}(\lambda,\theta_i,\varphi_i)$

Mobley [1] employed the widely used Hydrolight [3] to simulate $L_w(\theta_{v,w},\varphi)$, $L_t(\theta_{v,w},\varphi)$ and $L_{sky}(\theta_i,\varphi_i)$ for the evaluation of ρ, where "The semiempirical sky radiance model of Harrison and Coombes was used to define the angular pattern of the sky radiance distributions incident onto the sea surface." However, the model of Harrison and Coombes [4] is for "short (0.3-3.0 μm) … wavelength regions", not for spectrally resolved $L_{sky}(\lambda,\theta_i,\varphi_i)$. To generate $L_{sky}(\lambda,\theta_i,\varphi_i)$ for an arbitrary incident direction (θ_i,φ_i) in Hydrolight, the same spatial distribution function developed for broadband radiance [4] is used for radiance of a wavelength. Consequently, for L_{sky} from two different directions, the ratio of $L_{sky}(\lambda,\theta_i,\varphi_i)$ to $L_{sky}(\lambda,\theta_j,\varphi_j)$ is spectrally flat (see Fig. 1a for examples). When this spectrally flat relationship is applied to Eq. 5, it will result in a spectrally independent ρ for any given $(\theta_{v,w},\varphi)$, which is likely the reason that the ρ value in Mobley [1] was

not specified for any wavelength. This is contradictory to that ρ is "… wavelength dependent" [1], and it is not consistent with observations for a clear-sky day (see Fig. 1b). Note that, based on Eq. 5, if $L_{sky}(\lambda,\theta_{v,s},\varphi)$ is from 40°/135°, but $L_{sky}(\lambda,\theta_i,\varphi_i)$ include sky radiance from near horizon (see the brighter pixels in Fig. 2), ratio of $L_{sky}(\lambda,\theta_i,\varphi_i)/L_{sky}(\lambda,40^o,135^o)$ could increase significantly with the increase of wavelength, and then may result in a ρ increases with wavelength [5, 6]. Because the Harrison and Coombes model cannot simulate the distribution of spectral sky radiance, which is critical in forming spectral L_{srs}, the recommended 0.028 of ρ value for the 40°/135° observation geometry might be only appropriate for a specific wavelength (which is not known yet), rather a general value for the calculation of spectral R_{rs}.

b) Wave slopes at L_t measurements vs. the average wave slope of the Cox-Munk model

Another factor affecting the evaluation of ρ is the modeling of the waves (for the estimation of W_i) on the wind-roughened sea surface. Fig. 2 is a picture of commonly observed surface patterns in the ocean, clearly showing many waves with different orientations and wave slopes (or wave heights) that form the wave facets reflecting L_{sky} from a wide range of directions into sensor's FOV at a given time. Hydrolight employed the Cox-Munk model [7] of the wave slopes, but this model was developed based on aerial photographs taken at an altitude of 2000 ft that covered a surface area roughly 300,000 m^2, which is much larger than the yellow rectangle area in Fig. 2. However, when L_t is measured with a spectrometer in the field via AWA, the altitude is ~10 m. For a sensor with an FOV of ~10 degree, it sees a surface area roughly 1 m^2. Because the wind-roughened surface is so complex (see Fig. 2), each small area (the red circles, for example) has its own major wave slopes. Thus, to match the average status of Cox-Munk's model, it is necessary to take 100's of thousands of L_t scans or to have a very long integration time, and then take an average. This kind of measurement requirement can hardly be met in taking field measurements for R_{rs}. Thus, the average wave pattern of the Cox-Munk model does not necessarily match the wave pattern corresponding to an L_t scan in AWA. Note that it is mainly the different wave patterns causing the variations (sometimes quite large) of measured L_t under the same geometry within a short time span even under cloudless conditions.

Separately, the relationship between wind speed and wave slopes developed by Cox and Munk [7] was based on measurements in deep oceanic water, where the waves are deep-water waves. For shallow waters (such as many inland lakes), this wind-wave relationship is not necessarily applicable, thus the ρ vs wind speed table [1], even assume it is appropriate, is not necessarily applicable for shallow waters.

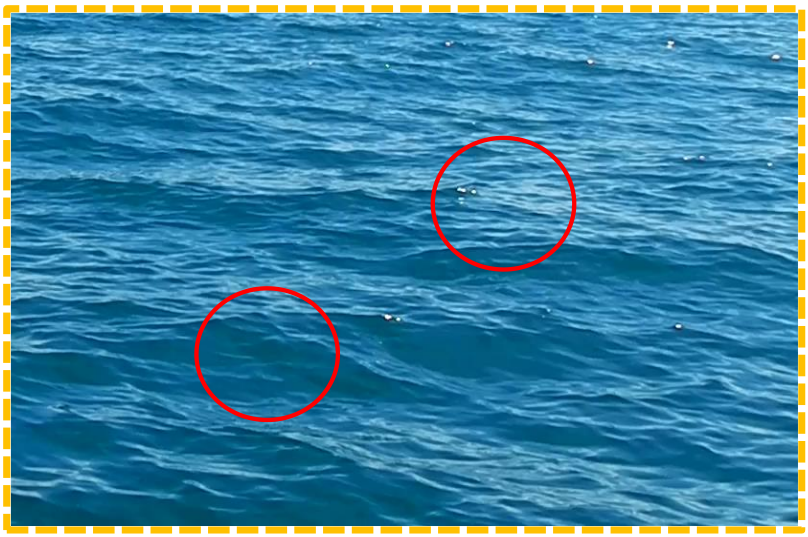

Fig. 2. A photograph (under cloudless sky) shows the wide range of wave heights (or slopes) of wind-roughened sea surface. When a radiance sensor measures L_t, it is a very small portion constrained by the FOV of the radiance sensor (e.g., the red circles) compared to the rectangular (yellow dash line) area. (Photo credit, Zhongping Lee).

3. The workaround to calculate R_{rs} from measurements via AWA

From the above discussions, it is clear that if formula Eq. 4 is used to calculate R_{rs}, it is necessary to employ spectrally varying ρ values for each viewing geometry, rather a fixed value as suggested in Mobley [1]. Further, based on Eq. 5, it is also clear that for each L_t scan, it is difficult, if not impossible, to accurately estimate its corresponding ρ spectrum. To work around this dilemma so an R_{rs} spectrum could be generated from the AWA measurements, the equation for the calculation of R_{rs} is commonly approximated as [5, 8]

$$R_{rs}(\lambda,\theta_{v,w},\varphi) = \frac{R_g(\lambda)}{\pi}\frac{\left(L_t(\lambda,\theta_{v,w},\varphi) - f(\theta_{v,w},\varphi)L_{sky}(\lambda,\theta_{v,s},\varphi)\right)}{L_g(\lambda)} - \Delta \quad (6)$$

Here the two parameters, f and Δ, are assumed spectrally independent, with f the Fresnel reflectance of sea water for viewing angle ($\theta_{v,w}$,φ). Δ represents a lump sum of the "residual" sky glint and sun glint (see the bright glitter in Fig. 2), which in theory is also wavelength dependent [2][9]. This expression basically assumes that the spectrally varying part of L_{srs}/E_s mainly comes from the specular reflectance of $L_{sky}(\lambda,\theta_{v,s},\varphi)$, while the sum of all the other contributions is spectrally flat when ratioed to E_s. Note that Groetsch et al. [9] proposed a more sophisticated formulation where spectrally varying Δ is used to reflect the residual sea-surface contributions.

The value of f can be calculated from the Fresnel law by assuming a flat sea surface, while the value of Δ has to be determined through other approaches [5, 9-12], and this latter correction is termed as "residual reflectance corrections" in the NASA protocol [13] for the measurement of R_{rs} via AWA. In short, for the determination of R_{rs} from measurements via AWA, a spectrally constant ρ value along with formula by Eq. 4 is not supported by the nature of reflected sky radiance by

roughened sea surface, which will result in large uncertainties in the R_{rs} product. The formula by Eq. 6 along with the various proposed processing procedures, although not perfect, would provide a better determination of R_{rs} for AWA.

4. Further considerations

a) Polarization

In the above discussions, there is no consideration of the polarization status of radiance. Natural light fields, particularly skylight, are polarized. Even if the sensors deployed in AWA are designed insensitive to polarization, the state of polarization of incident light affects the total energy reflected. If a radiative transfer model that is used to simulate ρ does not include polarization, ρ will be underestimated with the degree of underestimation dependent on the solar zenith angle, aerosol concentration, wind speeds [2, 14]. This polarization effect also varies spectrally, decreasing with increasing wavelength. On average, ignoring polarization would lead an underestimation of ρ by 8-20% at 400 nm to 0-10% at 1000 nm. Note that polarization only affects ρ due to skylight, which is polarized, and does not affect ρ due to the direct sunlight, which is unpolarized.

b) Ambient light field

Because AWA with one spectrometer takes consecutive measurements of three components (L_g, L_t, L_{sky}), a key requirement for this field-measurement setting is a stable ambient light field, otherwise the ratio showing by Eq. 4 or Eq. 6 is not valid. This requirement places a big challenge for cloudy days, where it is common to encounter an environment in which the clouds are changing rapidly. Also, for earlier morning and late afternoon, the incident radiation from the Sun varies a lot, it is thus necessary to complete the measurements in a very short time even for cloudless environments. One option to overcome varying ambient light field is to employ three spectrometers, with each one assigned for a specific component and taking all the measurements simultaneously. This will require all the sensors be well calibrated and places a greater financial burden.

5. The hardware approach for accurate measurement of R_{rs} in the field

To bypass the complex processing as shown by Eq. 6 and the uncertainties associated with AWA, a more robust scheme is to use a hardware to mechanically block surface-reflected light [15, 16], i.e., the skylight blocked approach (SBA). Studies [17] have shown that, after correcting the self-shading effect (which is less than 3% for blue waters in the blue wavelengths for a cone with 10 cm in diameter), SBA can provide highly accurate R_{rs} in all natural aquatic environments.

6. Concluding remarks

Due to many out-of-control factors, accurate determination of R_{rs} in the aquatic environment is far from easy. The above-water-approach (AWA) is easy to be carried out, but it is necessary to be very careful in its post-measurement data processing, where the formulation of Eq. 4 along with

a spectrally constant ρ value may not result in accurate R_{rs} spectra from AWA. For better results from AWA, it is necessary to take a more sophisticated data processing scheme.

References

1. Mobley, C.D., *Estimation of the remote-sensing reflectance from above-surface measurements.* Applied Optics, 1999. **38**: p. 7442-7455.
2. Zhang, X., S. He, A. Shabani, P. Zhai and K. Du, *Spectral sea surface reflectance of skylight.* Optics Express, 2017. **25**(4): p. #275869.
3. Mobley, C.D. and L.K. Sundman, *HydroLight 5.2 User's Guide*. 2013, Bellevue, Washington.: Sequoia Scientific, Inc., https://www.numopt.com/hydrolight.html.
4. Harrison, A. and C. Coombes, *An opaque cloud cover model of sky short wavelength radiance.* Solar Energy, 1988. **41**(4): p. 387-392.
5. Lee, Z.-P., Y.-H. Ahn, C. Mobley and R. Arnone, *Removal of surface-reflected light for the measurement of remote-sensing reflectance from an above-surface platform.* Optics Express, 2010. **18**(25): p. 26313-26342.
6. Cui, T.W., Q.J. Song, J.W. Tang and J. Zhang, *Spectral variability of sea surface skylight reflectance and its effect on ocean color.* Opt. Exp., 2013. **21**: p. 24929-24941.
7. Cox, C. and W. Munk, *Measurement of the roughness of the sea surface from photographs of the Sun's glitter.* Journal of the Optical Society of America, 1954. **44**(11): p. 838-850.
8. Carder, K.L. and R.G. Steward, *A remote-sensing reflectance model of a red tide dinoflagellate off West Florida.* Limnol. Oceanogr., 1985. **30**: p. 286-298.
9. Groetsch, P., P. Gege, S. Simis, M. Eleveld and S. Peters, *Validation of a spectral correction procedure for sun and sky reflections in above-water reflectance measurements.* Optics Express, 2017. **25**(6): p. #286475.
10. Ruddick, K.G., V.D. Cauwer, Y.-J. Park and G. Moore, *Seaborne measurements of near infrared water-leaving reflectance: The similarity spectrum for turbid waters.* Limnology and Oceanography, 2006. **51**(2): p. 1167-1179. DOI: 10.4319/lo.2006.51.2.1167.
11. Kutser, T., E. Vahtmäe, B. Paavel and T. Kauer, *Removing glint effects from field radiometry data measured in optically complex coastal and inland waters.* Rem. Sens. Envi., 2013. **133**: p. 85-89.
12. Zibordi, G., S.B. Hooker, J.F. Berthon and D. D'Alimonte, *Autonomous above-water radiance measurements from an offshore platform: A field assessment experiment.* Journal of Atmospheric and Oceanic Technology, 2002. **19**(5): p. 808-819.
13. Mueller, J.L., G.S. Fargion and C.R. McClain. *Ocean Optics Protocols For Satellite Ocean Color Sensor Validation, Revision 4*. 2003. Goddard Space Flight Center, Greenbelt, MD: NASA.
14. Mobley, C.D., *Polarized reflectance and transmittance properties of windblown sea surfaces.* Appl. Opt., 2015. **54**(15): p. 4828–4849.
15. Tanaka, A., H. Sasaki and J. Ishizaka, *Alternative measuring method for water-leaving radiance using a radiance sensor with a domed cover.* Optics Express, 2006. **14**(8): p. 3099-3105.
16. Lee, Z.-P., N. Pahlevan, Y.-H. Ahn, S. Greb and D. O'Donnell, *A robust approach to directly measure water-leaving radiance in the field.* Applied Optics, 2013. **52** (8): p. 1693-1701.
17. Wei, J., M. Wang, Z. Lee, M. Ondrusek, S. Zhang and S. Ladner, *Experimental analysis of the measurement precision of spectral water-leaving radiance in different water types.* Optics Express, 2021. **29**: p. 2780-2797.

Acknowledgements

Comments and suggestions by Dr. Curtiss Mobley are greatly appreciated. We thank Keping Du for providing simulated sky radiance by Hydrolight, Shuguo Chen, Cheng Xue, Gong Lin, Liangfeng Chen, Wendian Lai, and Siyuan Hou for providing measured sky radiance.